stressed state at a given time [2-5]. Some studies have observed a decrease in the yield strength with an increase in the degree of hydrogen charging [6,7]. Furthermore, one theory of hydrogen embrittlement, known as hydrogen-enhanced localized plasticity (HELP), claims that reduction in the overall ductility under the action of hydrogen occurs due to facilitated plastic deformation at the crack tip [8,9].

These facts must be taken into account in strength analysis during the long-term operation of steel structural elements in aggressive hydrogen-containing environments. The hydrogen-induced change in the properties of some steels is manifested as hydrogen embrittlement, i.e., a decrease in the ductility of the material as it is saturated with hydrogen. No universal model has been constructed so far to produce reliable forecasts for the lifetimes of structures taking into account the embrittlement of the material. This is also a crucial issue for strength analysis of steel pipes transporting the so-called sour gas, i.e., natural gas with increased content of hydrogen sulfide. Since strong hydrogen charging of metal occurs in environments containing hydrogen sulfide, pores filled with hydrogen are produced in the steels, leading to delamination. Predicting the behavior of such metal structures is a major problem that is yet to be addressed definitively.

This paper proposes a method for determining the strength of a metal shell structure under mechanical loading taking into account prolonged contact with an aggressive environment containing hydrogen sulfide. Since it is difficult to conduct long-term experimental studies of the material for the whole variety of possible load combinations that can affect the structure during operation, the model representation was based on the extrapolation of mechanical parameters. The method is illustrated in the case of a cylindrical steel pipe used for wells and gas collection systems of pipelines.

The problem of determining the long-term strength in thin-walled metal structures consists of several independent problems of applied mechanics, mathematical physics, and materials science. The general problem can be represented as:

– determining the stressed state in the given structural element;

– determining the mechanical parameters, depending on the saturation time of the material specimens with hydrogen sulfide;

– extrapolating the mechanical properties of the material to the potential lifetime of the structure;

– selecting the strength criterion and determining the instant in the lifecycle of the structure when the limit state occurs.

2. Materials and methods

Determination of the stressed state. We assume that the thin-walled structure considered is a shell of revolution with a thickness of h and a length of L, with variable geometric and mechanical parameters along the generatrix. Let us relate the shell to a middle surface determined by curvilinear orthogonal coordinates s, θ, γ, where s is the meridional coordinate, θ is the circumferential coordinate, and the coordinate γ is measured in the direction of the outer normal to the shell surface.

There are diverse computational programs for determining the stress state in thin-walled structures based on various numerical methods. Mathematical formalization of the problems is typically based on a specific shell theory. In this paper, we rely on the classical shell theory based on the Kirchhoff–Love hypotheses to determine the stress-strain state of a thin-walled structure [10]. The stress-strain state of an arbitrarily loaded shell of revolution is described by a system of eight partial differential equations [10-12]

$$\partial \bar{Y}/\partial s = \sum_m A_m(s,\theta)\partial^m \bar{Y}/\partial \theta^m + \bar{f}(s,\theta),\ (s_0 \le s \le s_L) \quad (1)$$

with the boundary conditions

$$B_1\bar{Y}(s_0) = \overline{b_1},\ B_2\bar{Y}(s_L) = \overline{b_2}. \quad (2)$$

Here $\bar{Y}$ is the vector of the required solution; $\bar{f}$ is the vector whose components depend on the loads applied to the shell; B_1 and B_2 are the given matrices; $\overline{b_1}$ and $\overline{b_2}$ are the given vectors; the elements of the matrix A_m depend on the geometric and mechanical characteristics of the shell.

The internal surface of the shell comes into contact with the aggressive hydrogen-containing environment with the excess pressure *p*. Considering that the shell considered is loaded only with a pressure *p* during operation, its stress-strain state is axially symmetrical. The stressed state under axisymmetric deformation of the shell can be determined by integrating a system of six ordinary differential equations [13-16]

$$d\bar{Y}/ds = P_{ij}\bar{Y} + \bar{f} \quad (3)$$

with the vector of the solution

$$\bar{Y} = \{N_r, N_z, M_s, u_r, u_z, \vartheta_s\}, \quad (4)$$

where N_r, N_z are the radial and axial forces; u_r, u_z are the displacements; M_s is the meridional bending moment; ϑ_s is the normal rotation angle.

Discrete orthogonalization developed by S. Godunov [10,17,18] is applied to solve the linear boundary-value problem (3): this method 'normalizes' the solution and is used to solve various problems for shell structures [10-16]. The boundary-value problem solved by accounting for plastic deformation becomes nonlinear. The nonlinear problem is solved by the method of elastic solutions proposed by Ilyushin [19]. The method for linearization of the problem is considered in detail in [13,15]. The volumetric stress state of the shell is compared with the uniaxial state under simple stretching of the specimen.

$$S = \sigma/\sqrt{3},\ H = \varepsilon(1+\mu^*)/\sqrt{3}, \quad (5)$$

where σ and ε are the stresses and strains under simple stretching of the specimen, μ^* is the coefficient of transverse deformation, defined as in [13,14]

$$\mu^* = 0.5 - \sigma(1-2\mu)/2E\varepsilon, \quad (6)$$

where *E* is the elastic modulus; μ is Poisson's ratio. The intensities of shear stresses *S* and shear strains *H* for the shell are given as

$$S = \sqrt{(\sigma_s^2 + \sigma_s\sigma_\theta + \sigma_\theta^2)/3}, \quad (7)$$

$$H = \sqrt{\left[(\varepsilon_s - \varepsilon_\gamma)^2 + (\varepsilon_\gamma - \varepsilon_\theta)^2 + (\varepsilon_\theta - \varepsilon_s)^2\right]/6}, \quad (8)$$

where σ_s and σ_θ are the meridional and circumferential stresses, respectively; ε_s, ε_θ and ε_γ are the strain components along the meridian, circumference, and normal to the surface of the shell.

The meridional and circumferential stresses $\sigma_s(\gamma)$, $\sigma_\theta(\gamma)$ and the corresponding strains $\varepsilon_s(\gamma)$, $\varepsilon_\theta(\gamma)$, as well as the intensities of shear stresses $S(\gamma)$ and shear strains $H(\gamma)$ are determined at each point of the shell after integration of system (3).

Mechanical parameters of the material. The stress state of the given structure is established by finding the mechanical parameters of the material depending on the time of saturation with hydrogen sulfide. The problem of hydrogen diffusion into the metal wall of the shell was solved in [16], determining the distribution of hydrogen concentration as a function of time for bodies of revolution [16]. Considering shells with a small wall thickness, we assume that hydrogen concentration along the thickness is the same. This hypothesis is confirmed by computational experiments for thin-walled structures, with a long period of hydrogen charging [16]. Therefore, the change in the mechanical parameters of the shell material depends only on the time *t* of saturation with hydrogen sulfide.

To illustrate the method for determining the strength of thin-walled structures, we examine shells of 12GB pipe steel, whose mechanical characteristics change under contact with an aggressive hydrogen sulfide medium. Measurements of the mechanical characteristics

in 12GB pipe steel specimens exposed to hydrogen sulfide for 96–384 hours are given in [20], along with measurements for specimens in the initial state, directly under uniaxial tensile stresses up to failure. Potential plastic deformations of the structure can be taken into account by obtaining stress-strain curves for this material $\sigma = f(\varepsilon, t)$ with the specimens stretched in the initial state and after hydrogen charging. These curves can be fitted fairly accurately by bilinear lines with points of yield strength $(\sigma_Y, \varepsilon_Y)$ and ultimate tensile strength $(\sigma_{ult}, \varepsilon_{ult})$ for different times t of contact with an aggressive environment, where σ_{ult} and ε_{ult} are the maximum stresses and strains under fracture. Table 1 shows the coordinates of the points for constructing such diagrams.

Table 1. Coordinates of points for approximating the diagrams $\sigma = f(\varepsilon, t)$

Time, h	Point 1		Point 2		Point 3	
	ε_0	σ_0, MPa	ε_Y	σ_Y, MPa	ε_{ult}	σ_{ult}, MPa
0	0	0	0.00187	374	0.23	474
96	0	0	0.00181	361	0.22	458
192	0	0	0.00213	426	0.14	498
384	0	0	0.00218	437	0.12	500

Figure 1 shows one of the diagrams corresponding to the initial state of the specimen material. Squares correspond to experimental data from [20].

Extrapolation of mechanical properties of the material. Stresses and strains during the time range for which the specimen is saturated with hydrogen sulfide can be determined by interpolation. The change in the mechanical parameters of material under saturation with hydrogen sulfide can be extrapolated beyond the experimental time range t_{exp} to the structure's period of safe operation t_w.

We accept the hypothesis that the physico-chemical processes in the metal exposed to hydrogen sulfide are monotonic. Therefore, the change in the mechanical parameters of the material during contact with hydrogen sulfide can be extrapolated beyond the experimental time range. Apparently, extrapolation is correct up to a time comparable to the time in which the experiment was conducted with the same conditions for temperature and loading and within the limits of the same type of failure. However, it is suggested in [21] that extrapolation can be also applied for a time exceeding the maximum durability (for which the rupture strength curves were experimentally obtained) by an order of magnitude.

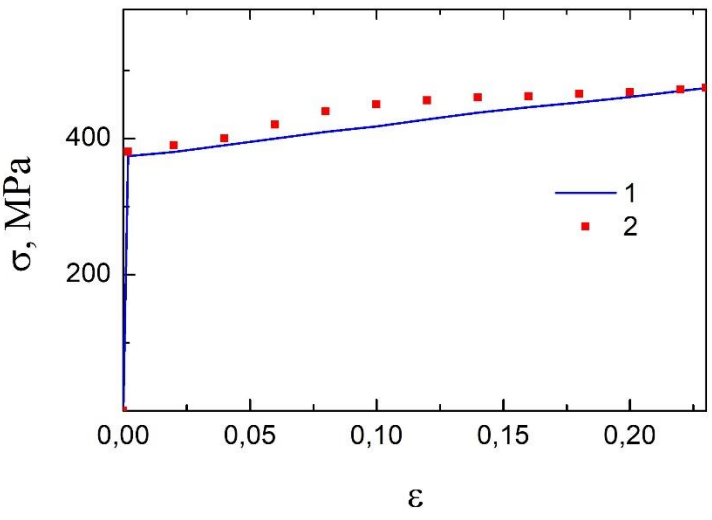

Fig. 1. Approximated diagram $\sigma = f(\varepsilon, 0)$

Different variants of neural networks can be used to calculate the required values outside the experimental time range. Neural networks can be used in various fields of science and technology due to their approximating capabilities and the options for calculating different nonlinearities [22,23]. After training, the network can predict the future value for some sequences based on several previous values of existing factors. At the training stage, the neural network reconstructs the target function from a set of training samples, that is, solves the problem of interpolation. The trained neural network can use the reconstructed dependence to obtain the predicted value and solve the extrapolation problem. This method of neural networks is integrated into the later versions of the Wolfram Mathematica 11.3 package for symbolic calculations.

Determination of the structure's operating time. We assume that the limit state of the structure occurs during long-term operation when the strength criterion of the material is violated at the most loaded point of the shell. This instant determines the structure's time of safe operation t_w. The condition commonly taken as the strength criterion of the structural material in the volumetric stress state is that the intensity of shear stresses (7) at the most loaded point of the shell reaches the uniaxial stresses for the specimen $\sigma_{ult}/\sqrt{3}$ during fracture.

In accordance with the well-known scheme constructed by Ioffe, a decrease in temperature is accompanied by a decrease in the ductility of the metal up to embrittlement [24]. A similar phenomenological effect is observed with an increase in hydrogen concentration during electrochemical hydrogen charging in steels. The yield strength σ_Y and the ultimate tensile strength σ_{ult} depend on the concentration of hydrogen sulfide, and, therefore, on the operating time t of the shell structure. The constructed kinetic curves $\sigma_Y(t)$ and $\sigma_{ult}(t)$ approach each other for many materials, converging at a time $t = t_{BR}$ in the point $\sigma_Y(t_{BR}) = \sigma_{ult}(t_{BR})$ [25]. This time point in the operating cycle separates the ductile fracture range in the material from the brittle fracture range. However, this condition only holds true for a local zone with plastic deformation and maximum intensity of shear stresses.

Thus, the following condition can be used as the criterion for the rupture strength of structures under constant loading:

$$S(t) = \sigma_{ult}(t)(\sqrt{3})^{-1}. \quad (9)$$

Violation of condition (9) determines the permissible operating time of the shell and its lifetime.

3. Results and discussion

Let us determine the stress state and the strength of the cylindrical shell (pipe), operating in a hydrogen-containing medium for a long time. The outer diameter of the pipe is D = 0.114 m, the thickness is h = 0.013 m, the length is L = 1 m, and the material is 12GB steel (equivalent to X42SS steel according to the classification of the American Petroleum Institute). The pipe experiences a plane stress state from the alternating internal pressure p during operation. If we assume that the pipe is sufficiently long, boundary conditions (2) do not considerably affect the stress state in the section that interests us, $s = 0.5\,L$.

As noted above, by integrating a system of equations (3) at each point of the shell, we can determine the meridional and circumferential stresses and strains, as well as the intensities of shear stresses and shear strains at any internal pressure. At an overpressure of p = 80 MPa, the entire material of the shell is still in the elastic strain range, and the maximum intensity of shear strain H reaches $0.00111 < \varepsilon_Y$. Meridional and circumferential stresses σ_s = –7.04 MPa and σ_θ = 307.38 MPa act on the outer surface of the shell, σ_s = 0 and σ_θ = 309.5 MPa on the centerline, and σ_s = 7.04 MPa and σ_θ = 311.61 MPa on the inner surface. As a test, the obtained stresses were compared with the stress calculated for a shell loaded with internal

pressure using the momentless theory [26] $\sigma_\theta = pR_{cp}h^{-1} = 310.76$ MPa, where R_{cp} is the mid-radius of the shell. The results are in good agreement.

Table 2 gives the intensities of shear stresses $S = f(p)$ and shear strains $H = f(p)$ for the shell at different internal pressures p for $t = 0$ hours.

Table 2. Intensities of shear stresses and shear strains for t = 0 h

p, MPa	S, MPa	H
80	177.9	0.00111
90	200.0	0.00125
100	224.1	0.01962
110	248.8	0.09412
120	273.2	0.16724

When the overpressure p = 90 MPa is reached, plastic deformations occur at the most loaded point on the inner surface of the shell. The problem becomes physically nonlinear, and an iterative process is applied to obtain the given relative accuracy of 0.01 for the solution of the nonlinear problem [15].

Because the influence of hydrogen sulfide on the mechanical parameters of the material starts to manifest beyond the yield point σ_Y in the specimen's plastic strain range, we consider the kinetics of the stress state in the shell with p = 100 MPa, when plastic deformation zones appear near the most loaded point. Table 3 gives the intensities of shear stresses $S = f(t)$ and shear strains $H = f(t)$ for the shell with different operating times t of the structure in contact with hydrogen sulfide.

The given relative accuracy of the nonlinear problem for the operating time t = 0 h can be achieved in 86 approximations, 70 approximations are required for the time of 96 h, 3 approximations for 192 h, and only one approximation is sufficient for 384 h (the entire material of the shell is in the elastic range). Consequently, embrittlement of the shell material occurs at t = 384 h.

Table 3. Values S and H for p = 100 MPa

t, h	S, MPa	H
0	224.1	0.01962
96	224.9	0.04435
192	222.4	0.00142
384	222.4	0.00146
800	222.4	0.00142

It follows from Table 3 that the intensities of shear stresses S and shear strains H practically do not change during the operating time limited by the experiment.

A particular configuration of neural network was used to calculate the required values outside the experimental time range. A three-layer neural network from the Wolfram Mathematica 11.3 package with a hyperbolic tangent as an activation function was used in this study to interpolate and extrapolate the curves $\sigma_Y = f(t)$ and $\sigma_{ult} = f(t)$. Figures 2(a) and 2(b) show the yield strength σ_Y and ultimate tensile strength σ_{ult}, respectively, depending on the time limited by the experiment considering the influence of hydrogen sulfide on the metal. The experimental data from [20] are marked by points, the solid lines correspond to the interpolation values.

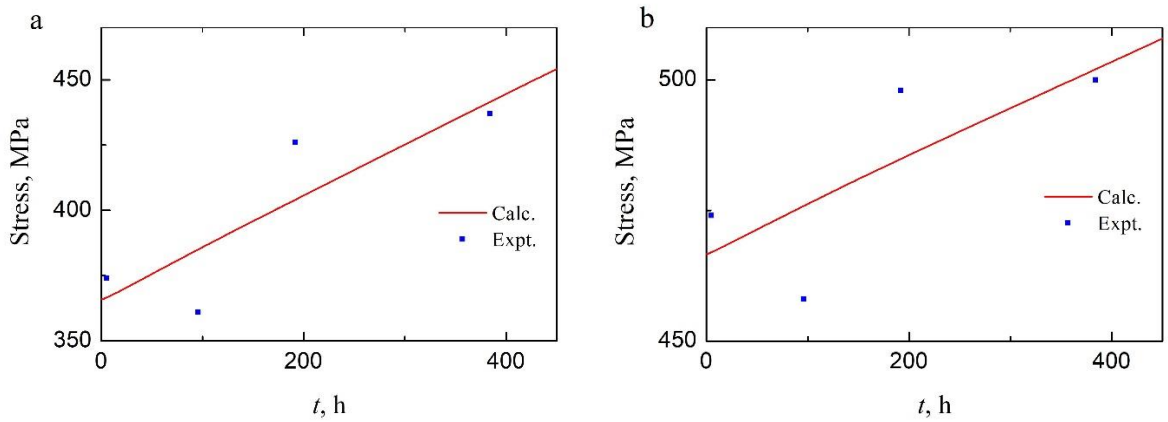

Fig. 2. Yield strength (a) and ultimate tensile strength (b) depending on the saturation time of the specimen with hydrogen sulfide

Figure 3 shows the variation in the yield strength (curve 1) and ultimate tensile strength (curve 3) during the time of contact between specimens and hydrogen sulfide up to 1000 hours. Evidently, the constructed kinetic curves $\sigma_Y(t)$ and $\sigma_{ult}(t)$ converge with a time close to t_{BR} =1000 h, $\sigma_Y(t_{BR}) = \sigma_{ult}(t_{BR})$.

If inequality $t > t_{BR}$ is satisfied, the steel considered becomes brittle and, therefore, the stress state and the strength condition can be determined within the framework of linear elasticity theory. If $t < t_{BR}$, then the physical equations describing the properties of steel should follow plasticity theory.

Thus, the stress-strain state of the shell for the particular operating time of the structure t^* = 800 hours can be determined using the kinetic curves $\sigma_Y(t)$ and $\sigma_{ult}(t)$, shown in Fig. 3. In this case, we obtain σ_Y^* = 510 MPa and σ_{ult}^* = 530 MPa.

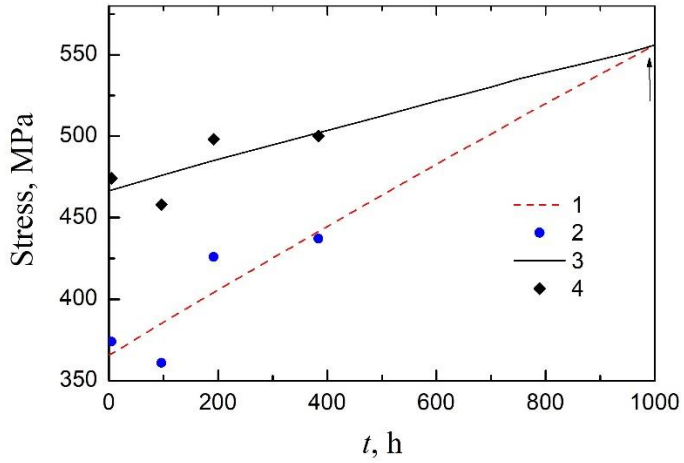

Fig. 3. Computational dependences of yield strength (curve 1) and ultimate stress (curve 3) on the contact time of the specimen with hydrogen sulfide. Dots and squares correspond to experimental values [20]

The approximated diagram $\sigma = f(\varepsilon, t^*)$ for t^* = 800 h can be constructed by finding ε_Y^* and ε_{ult}^*. Given that Young's modulus E practically does not change when the specimens are saturated with hydrogen sulfide, the yield-point strain is $\varepsilon_Y^* = \sigma_Y^* E^{-1} = 0.00255$. The fracture strain beyond the elastic limit consists of two components: elastic and residual δ. Therefore, when the specimen is fractured, the relative ultimate strain is defined as $\varepsilon_{ult}^* = \sigma_{ult}^* E^{-1} + \delta^*$.

Figure 4 shows the variation of residual strain $\delta(t)$ over the contact time of the specimens with hydrogen sulfide up to t = 900 h. The points denote the experimental values $\delta(t)$given in [20]. Therefore, we have δ^* = 0.04 for time t = 800 h.

Thus, to determine the stress state for the operating time t^* = 800 h, the tensile curve should be approximated by a bilinear function with the points of yield strength σ_Y^* = 510 MPa, $\varepsilon_Y^* = 0.00255$ and ultimate tensile strength σ_{ult}^* = 530 MPa, ε_{ult}^* = 0.04265. After integrating the system of equations (3) at each point of the shell, we can easily find the necessary components of stress and strain at any value of internal pressure. Table 3 shows the intensities of shear stresses *S* and shear strains *H* for the shell during the operating time of 800 hours.

Considering the point found for the operating time of t_{BR} =1000 h, which separates the ductile fracture range of the material from the brittle fracture range for the shell considered, two conditions should be imposed for strength. We assume that fracture of the shell for the operating time $t < t_{BR}$ (plastic strain range) occurs when the integral intensity of shear stresses $S_h(\gamma)$ at the most loaded point reaches the ultimate tensile stress σ_{ult} upon fracture of the specimen material.

$S_h = \sigma_{ult}\left(\sqrt{3}\right)^{-1}$,

where $S_h = [\int_{-h/2}^{h/2} S(\gamma)d\gamma]/h$ is the integral intensity of shear stresses in the shell.

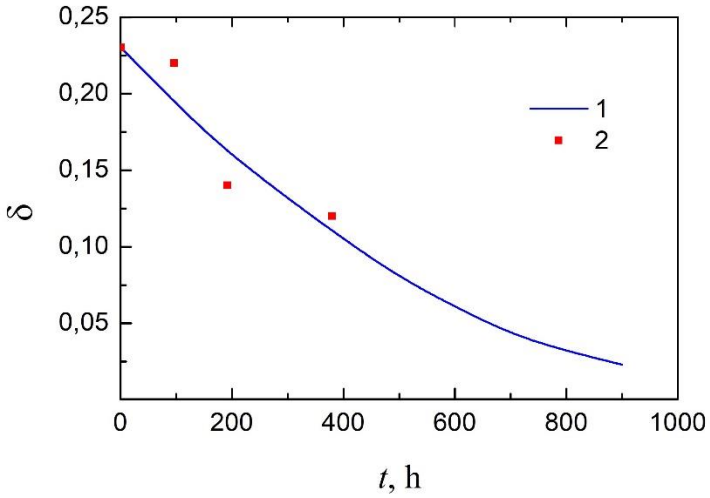

Fig. 4. Variation of residual strain

Fracture of the shell for the operating time $t > t_{BR}$ (brittle deformation range) occurs when the intensity of shear stresses *S* at the most loaded point reaches the ultimate tensile stress σ_{ult} upon fracture of the specimen material. The continuity of the material at the most loaded point of the structure is violated provided that (9).

4. Conclusion

The paper proposes a method for determining the stress state, strength, and lifetime of thin-walled structures exposed to aggressive environments containing hydrogen sulfide for prolonged periods, with estimates produced for the safe operation of the shell structure. The method is illustrated by an example of a cylindrical steel pipe used to transport hydrogen-containing gas mixtures.

The method is based on the hypothesis that the yield and ultimate tensile strengths of the specimen material depend on the time of contact with the hydrogen-containing environment. The mechanical parameters of the pipe material were determined using the data obtained during an earlier experiment in a limited time range. An increase in yield strength

and ultimate tensile strength was observed with an increase in the degree of hydrogen charging. We used extrapolation methods to obtain results suggesting that the yield and ultimate tensile strengths converge to a single point at longer operating times. This point of convergence allows us to establish which criterion should be used in strength analysis for the safe operation of shell structures. The brittle fracture criterion is applied for a time exceeding the value of the convergence point; otherwise, the criterion for shell strength under elastoplastic deformation should be used. Furthermore, no point of convergence may be observed for other materials, since the yield strength can decrease. Other representations will have to be adopted for the model in the calculations for these cases.

Thus, we established that the change in mechanical parameters can be described depending on the time of material exposure to hydrogen sulfide. The proposed criterion for the strength of the shell structure and the model for extrapolation of mechanical parameters beyond the experimental time range make it possible to determine the time in the life cycle of the structure, at which the limit state occurs.

References

[1] Olden V, Thurlow C, Johnsen R. Modelling of hydrogen diffusion and hydrogen induced cracking in supermartensitic and duplex stainless steels. *Materials and Design*. 2008;29(10): 1934-1948.

[2] Rebyakov YN, Chernyavskij AO, Chernyavskij OF. Deformation and fracture of materials and structures under diffusion conditions. *Vestnik SUSU.* 2010;10: 4-16. (In Russian)

[3] Jemblie L, Olden V, Akselsen O. A coupled diffusion and cohesive zone modelling approach for numerically assessing hydrogen embrittlement of steel structures. *International Journal of Hydrogen Energy*. 2017;42(16): 11980-11995.

[4] Fassina P, Bolzoni F, Fumagalli G, Lazzari L, Vergani L, Sciuccati A. Influence of hydrogen and low temperature on mechanical behaviour of two pipeline steels. *Engineering Fracture Mechanics*. 2012;81(2): 43-55.

[5] Pluvinagea G, Capelleb J, Meliani M. Pipe networks transporting hydrogen pure or blended with natural gas, design and maintenance. *Engineering Failure Analysis*. 2019;106: 104164.

[6] Chu WY, Li SQ, Hsiao CM, Ju SY. Effect of hydrogen on the apparent yield stress – research on the cause of hydrogen induced delayed plasticity. *Corrosion -Houston*. 1981;37(9): 514-521.

[7] Merson ED, Myagkikh PN, Klevtsov GV, Merson DL, Vinogradov A. Effect of hydrogen concentration and strain rate on hydrogen embrittlement of ultra-fine-grained low-carbon steel. *Advanced Structured Materials*. 2021;143: 159-170.

[8] Birnbaum HK, Sofronis P. Hydrogen-enhanced localized plasticity – a mechanism for hydrogen-related fracture. *Mater. Sci. Eng*. A. 1994;176(1-2): 191-202.

[9] Robertson IM. The effect of hydrogen on dislocation dynamics. *Eng. Fract. Mech*. 2001;68(6): 671–692.

[10] Grigorenko YM, Vasilenko AT. *Theory of Shells of Varying Stiffness. Vol. 4. Methods of Shell Design.* Kiev: Naukova Dumka; 1981. (In Russian)

[11] Vasilenko AT, Emelyanov IG. Determination of the Stressed State of Three-Layer Cylindrical Shells with Allowance for Layer Separation. *International Applied Mechanics*. 1999;35(5): 501-507.

[12] Vasilenko AT, Emelyanov IG, Kuznetsov VY. Stress Analysis of Laminated Shells of Revolution with an Imperfect Interlayer Contact. *International Applied Mechanics*. 2001;37(5): 662-669.

[13] Shevchenko YN, Babeshko ME, Piskun VV. *Solution of the axisymmetric thermoplastic problem for thin-walled and thick-walled bodies of revolution on a Unified Electronic Computer System*. Kiev: Naukova Dumka; 1980. (In Russian)
[14] Shevchenko YN, Prokhorenko IV. *Computational Methods for Shells. Vol. 3. Theory of Elastoplastic Shells with Noisothermal Loading Processes*. Kiev: Naukova Dumka; 1981. (In Russian)
[15] Emel'yanov IG. *Contact problems of the theory of shells.* Yekaterinburg: Ural Branch of the Russian Academy of Sciences; 2009. (In Russian)
[16] Emel'yanov IG, Mironov VI. Strength of Shell Structure Operating in Hydrogenous Media under Pressure. *Transportation Research Procedia*. 2021;54: 484-494.
[17] Godunov SK. Numerical solution of boundary-value problems for systems of linear ordinary differential equations. *Uspexi Matematicheskix Nauk*, 1961;16(3): 171-174. (In Russian)
[18] Grigorenko YM. Using Discrete Fourier Series to Solve Boundary-Value Stress Problems for Elastic Bodies with Complex Geometry and Structure. *International Applied Mechanics*. 2009;45(5): 469-513.
[19] Ilyushin AA. Plasticity. Fundamentals of general mathematical theory. Moscow: Publishing House of the Academy of Sciences of the USSR; 1963. (In Russian)
[20] Gorkunov ES, Zadvorkin SM, Veselov IN, Mitropol'skaya SY, Vichuzhanin DI. Influence of Uniaxial Tension on Magnetic Characteristics of the 12ÉÅ Pipe Steel Exposed to Hydrogen Sulfide. *Russian Journal of Nondestructive Testing*. 2008;44(8): 566-573.
[21] Troshchenko VT, Krasovsky AY, Pokrovsky VV, Sosnovsky LA, Strizhalo VA. *Strength of materials to deformation and destruction. Reference manual. Part 2*. Kiev: Naukova Dumka; 1994. (In Russian)
[22] Golubev YF. *Neural network methods in mechatronics*. Moscow: Mosk. Univ.; 2007 (In Russian).
[23] Aladjev VZ, Shishakov ML, Vaganov VA. *Mathematica: Functional and procedural programming*. 2rd ed. USA: KDP press; 2020.
[24] Ioffe AF. *Selected works. Vol. 1, Mechanical and electrical properties of crystals.* Leningrad: Nauka; 1974. (In Russian)
[25] Emel'yanov IG, Mironov VI, Lukashuk OA. Procedure for solving a physical-mechanical problem of determining stress fields, temperatures and hydrogen concentration. *AIP Conference Proceedings*. 2022; 2456(1): 020026.
[26] Pisarenko GS, Yakovlev AP, Matveev VV. *Handbook. Strength of materials.* Kiev: Naukova Dumka; 1988. (In Russian)

THE AUTHORS

Emelyanov I.G.
e-mail: emelyanov.ig.2016@mail.ru
ORCID: 0000-0002-9733-5485

Kislov A.N.
e-mail: a.n.kislov@urfu.ru
ORCID: 0000-0002-6600-7913